Sensing and Bio-Sensing Research 6 (2015) 85–89

Contents lists available at ScienceDirect

Sensing and Bio-Sensing Research

journal homepage: www.elsevier.com/locate/sbsr

A novel silicon based mags-biosensor for nucleic acid detection by magnetoelectronic transduction

Maria Eloisa Castagna [a,*], Salvatore Petralia [a], Maria Grazia Amore [a], Emanuele Cappello [b], Angela Beninato [c], Valentina Sinatra [b], Salvatore Baglio [c], Sabrina Conoci [a,*]

[a] STMicroelectronics, Stradale Primosole 50, 95121 Catania, Italy
[b] Distretto Micro e Nano sistemi, Ottava Strada, 5 -Zona Industriale, 95121 Catania, Italy
[c] DIEEI, Universita' degli Studi di Catania, Viale Andrea Doria, 95120 Catania, Italy

ARTICLE INFO

Article history:
Received 4 August 2015
Received in revised form 2 October 2015
Accepted 12 October 2015

Keywords:
Magnetic transduction
Nucleic acid amplification
Micro-heater
Temperature control

ABSTRACT

We developed a novel silicon biosensor based on magnetoelectronic transduction (MAGS) for nucleic acid detection. The mags-biosensor is a planar device composed by a primary micro-coil, and two secondary coils which produce a differential voltage due to the induced magnetic field. The presence of magnetic material over one of the secondary coils causes variations of induced magnetic field density that in turn results in a total output voltage different from zero. The voltage variation, therefore, is a measure of the amount of magnetic material present in the active zone. A device sensitivity of 5.1 mV/ng and a resolution of 0.008 ng have been observed. The biosensor also presents a micro-heater and a thermal sensor respectively to set and read-out the chip temperature: this aspect enables the device to be used for several biochemical applications that need temperature control and activation such for example nucleic acid amplification (real-time PCR), antigen- antibody detection (immune-assay) and SNP detection.

1. Introduction

Since its invention in the early 90s [1] real-time PCR has become an indispensable tool in many fields of molecular diagnostics, including determination of viral or bacterial loads in clinical samples, identification of germs in food, diagnosis of tumors, gene expression analysis, or forensic analyses [2]. The spread diffusion is due to the real time DNA amplification read out, thereby avoiding time-consuming post-PCR analysis.

Moreover, real-time PCR instruments currently on the market are based on complex and delicate optical components that lead to rather large, fragile and costly instruments, thereby restricting their use to specialized laboratories of analysis. The development of new miniaturized solutions for nucleic acids (DNA, RNA) analysis in portable and easy to use format (point-of-care), is one of the most important research pervasion of molecular analysis in the decentralized centers (hospitals, physician office).

Future point-of-care (PoC) molecular-level diagnosis requires advanced biosensing systems that can achieve high sensitivity and portability at low power consumption levels, all within a low price-tag for a variety of applications based on nucleic acids analysis such as epidemic disease control, biohazard detection, and forensic analysis. Several efforts have ears on the development of integrated optical components with high sensitivity to detect low fluorescent signals from small sample volume in order to miniaturize actual commercial instruments [3].

The interest in miniaturized biosensors is driving also the research efforts in finding electrical transduction mechanism. Biosensors development would be easier to produce (if made on Si-based devices and technologies) and to integrate in complex circuitries [4–6].

Magnetically labeled biosensors have been proposed as a promising solution for the miniaturization and integration and as candidate to potentially eliminate or augment the optical instruments used by conventional fluorescence-based sensors [7,8]. Magnetic detection methods require, in fact, minimal instrumentation, low electrical power supply and easily integration of both sensor element and circuitry in the same chip [8,9]. With respect to other types of markers (radioactive, enzymes, fluorophores, luminescent etc.), magnetic ones have many potential advantages: lower cost, higher stability, absence of toxicity, etc. Most of the applications employing magnetic beads devices have been focus on proteins detection (immune-assay). To the best of our knowledge there are only few examples in the literature that employ magnetic detection for nucleic acids [10,11].

In this paper, the proposed device, is basically a microtransformer constituted by a primary coil and two secondary coils connected in a differential configuration: the magnetic field generated by the

* Corresponding authors at: Stradale PrimoSole 50, 95125 Catania, Italy.
E-mail addresses: mariaeloisa.castagna@st.com (M.E. Castagna), sabrina.conoci@st.com (S. Conoci).

http://dx.doi.org/10.1016/j.sbsr.2015.10.003

primary coil, induces, at the secondary coils, voltages equal and opposite [9,12].

The presence of magnetic material over one of the secondary coils causes variations of induced magnetic field density that involves a total output voltage different from zero. The voltage variation, therefore, is a measure of the amount of magnetic material present in the active zone. The differential configuration has been chosen to filter undesired environmental noise: just one of the two secondary coils is made sensitive to the magnetic bead suitably functionalizing its surface.

The approach allows then an optimization of the device in terms of sensitivity [9,12].

In addition, biomolecules fixed to magnetic nanoparticles can be easily localized and manipulated by suitable magnetic fields.

The biosensor also presents a heater and a thermal sensor respectively to set and read-out the chip temperature: this aspect enables the device to be used for several biochemical applications that need temperature control, i.e. nucleic acid detection (Real Time PCR), immune-assay (antigen-antibody detection), SNP detection, host-guest detection etc.

The aim of this paper is to demonstrate the feasibility of integrated inductive magnetic sensors and their sensitivity to small amounts of magnetic beads, which is a promising characteristic for the future applications of the proposed approach to high-sensitivity, low-cost, portable biosensors. Also thermal components have been characterized and calibrated and its behavior in working regime analyzed.

2. Materials and method

2.1. Device fabrication

The thermal-magnetic sensor has been fabricated using conventional standard CMOS process technology. A high resistive silicon substrate (4500 Ω cm) has been chosen in order to minimize the loss of the magnetic field generated. Furthermore a thick silicon stoichiometric oxide (2 μm) has been thermally grown to electrically insulate the device from the substrate.

A first Aluminum (Al) metallization has been then sputtered in order to realize the thermal components, both heater and sensor. The thickness of the first metallization is 1 μm. A silicon oxide layer has been deposited and a mechanical planarization process has been implemented to avoid surface morphology: the residual oxide thickness in metal strips is 0.3 μm. After the planarization a dry etch has been performed to connect the first and the second metallization where necessary (i.e. on interconnection tracks).

The primary winding has been realized in the second metal layer (Al). The Al thickness (2.5 Am) has been chosen in order to regulate the current circulating in the primary coil and then the magnetic field generated. Again a silicon oxide has been deposited and planarized and then a third metal (Al) sputtered (1 μm) to define the secondary coils.

The dielectric layers thicknesses between metals have been maintained thinner than 0.3 μm to minimize effects of capacitive couplings.

Also metal 2 and metal 3 are connected through a vertical dry etch where necessary. Finally metal 3 is planarized through a deposited silicon oxide layer with residual thickness 0.3 μm and a 700 nm silicon nitride layer. The nitride, as passivation layer, has been selected to be roughness to chemical process necessary for the surface funzionalization required by application. The residual oxide and the nitride are removed just on the region to contact the device (see Fig. 1).

Fig. 2 shows the device layout with and without the heater ad thermal sensor (cyan layer).

The dimension of the whole die is 2400 μm × 2400 μm. The secondary coils present opposite winding sense; therefore, the resulting output voltage, which is the difference between the voltages across the secondary coils, is zero when no magnetic particles are present. Working

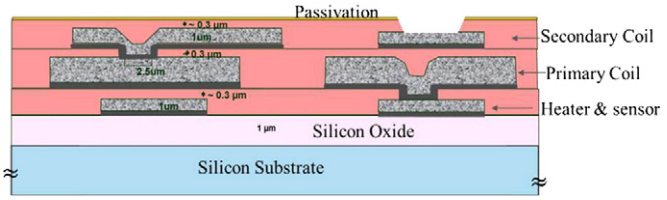

Fig. 1. Schematic cross-section of the device.

frequencies well below the RF range have been assumed as design constraint in order to simplify the readout circuitry that would be less sensitive to external interferences than in the case of high-frequency circuits. Moreover, from the point of view of the application as a biosensor, low-frequency operations would avoid possible alterations of the biological samples. The chip presents anyway a guard ring to shield environmental interferences.

The geometric and electric parameters of the planar microtransformers are summarized in Table 1. The inductance values have been calculated by using a modified Wheeler equation [13].

2.2. Device characterization

SEM images were obtained using a high-performance Schottky field emission LEO 1550 SEM Instrument operating at 5 kV in secondary-electron imaging mode.

The thermal-electrical characterization has been carried out by Karl Suss probe station with a thermal chuck (ModelPA200). The chuck temperature can be regulated from −40 °C to 160 °C. The electrical data have been acquired by using a Semiconductor Parameter Analyzer 4155C.

The experimental characterization has been perfomed in uniform temperatures conditions across the wafer thanks to the use of the heated chuck allowed the uniformity and distribution on wafer.

A Fluke thermocamera has been for thermal images acquisition.

ScreenMAG-Amine beads have been purchased by Chemicell GmbH. These beads are magnetic fluorescent silica particles with Hydrodynamic Diameter of 1.0 μm, core in Maghemite and matrix in non-porous Silica.

The device surface was treated with a specific chemical process to guarantee a good spot morphology and to create a coating suitable for further molecular grafting. In particular the device was cleaned by a plasma-O_2 process (Semitech equipment) for 10 min, with a plasma power of 100 W, and the cleaned surface properly silanized by an epoxy silane reagent by using a vapor phase process at 120 °C for 2 h in vacuum condition.

The deposition of microbeads on the surface of the secondary coils was carried out through a microspotter (Perkin Elmer piezo spotter) that allows the spotting of drops of 333 ± 43 pl. Microbeads solution at concentration of 12.5 mg/ml dispersed in sodium diphosphate 150 mM printing buffer (pH 9.2) containing an amount of 3×10^{-3}% of glycerol was employed. A number of spotted drops ranging from 3 to 60 corresponding to microbeads equivalent weight from 12 ng to 250 ng were deposed.

3. Results and discussions

Fig. 3 shows the device SEM cross-section in two different regions of the wafer. As respect to the geometrical dimensions reported in Table 1, we have observed a reduced track height and width for the primary coil: this feature has involved an enhancement in the primary coil resistance and inductance, respectively 1050 Ω and 3200 nH, and then a limitation in the maximum current flow, but not in the sensor working performances.

The comparison between the two images of Fig. 3 shows a good uniformity on wafer and a very good planarization process and thickness

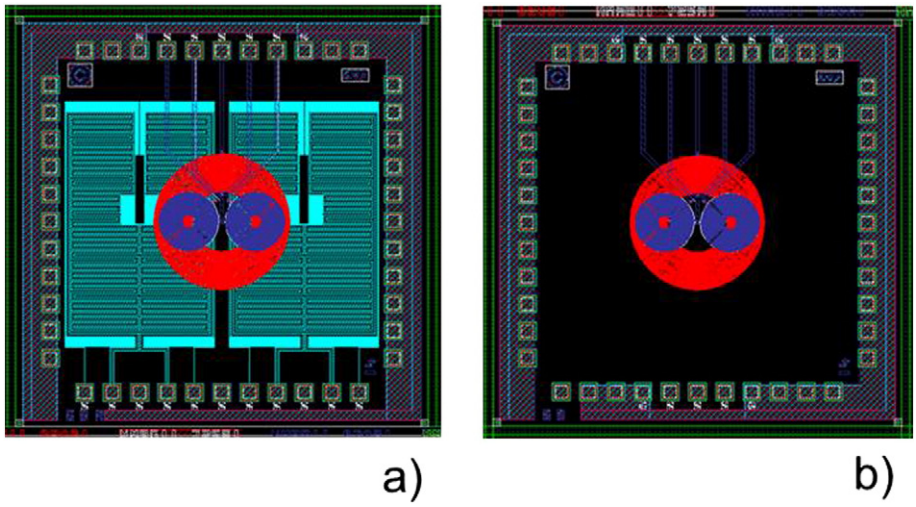

Fig. 2. Device layout with (a) and without (b) heater and thermal sensor.

Table 1
Geometrical and electric features of the transformer.

	Primary coil	Single secondary coil
Number of turns	56	45
External diameter	794 μm	267 μm
Internal diameter	349 μm	24 μm
Track height	2.5 μm	1 μm
Track width	2.5 μm	1.5 μm
Separation between tracks	1.5 μm	1.5 μm
Separation between coils	0.3 μm	
Inductance	2130 nH	54 nH
Series DC resistance	440 Ω	550 Ω

control of the dielectric layers among metallization layers. Moreover no voids are present between primary or secondary tracks.

The sensor characterization has been distinguished in the characterization of thermal and magnetic components due to the necessity to differently assembly the device.

3.1. Thermal components calibration and characterization

The development of biological applications requires the control of temperature, either in terms of profile (homogeneous or gradient) or in terms of the accessible range, and in both cases with the greatest accuracy possible. Indeed, the regulation of temperature is a critical parameter in managing many physical, chemical and biological applications. The micro-heater integration allows establishing a uniform temperature or a constant gradient in a given region. The integration of the thermal sensor increases control and accuracy of the temperature in the reaction chamber. Of course both elements have to be calibrated.

As can be observed in Fig. 2, the microheater and the thermal sensor are distinguished in two branches, correspondent to the secondary windings, that can work independently or in series, to maximize the thermal distribution on the whole chip. In order to be more sensitive to temperature cycling, the thermal sensor has been designed to have a resistance value 10 times greater than the micro-heater resistance. Fig. 4 reports both the resistance average values for sensor and heater versus chuck temperature in a range from 25 °C to 100 °C.

By using Eq. 1 both the resistance values for heater and sensor at 0 °C and the temperature coefficient have been calculated and reported in Table 2.

$$R = R_0[1 + \alpha(T - T_0)] \quad (1)$$

After the calibration on wafer, the device has been diced and assembled on a PCB board (Fig. 5a) in order to thermally insulate the device and, then, verify the temperature reached in the device by biasing the micro-heater. The image acquired by the thermocamera (Fig. 5b) shows the medium temperature (about 115 °C) of the chip biased at 6 V. To evaluate the thermal distribution on the chip a thermal

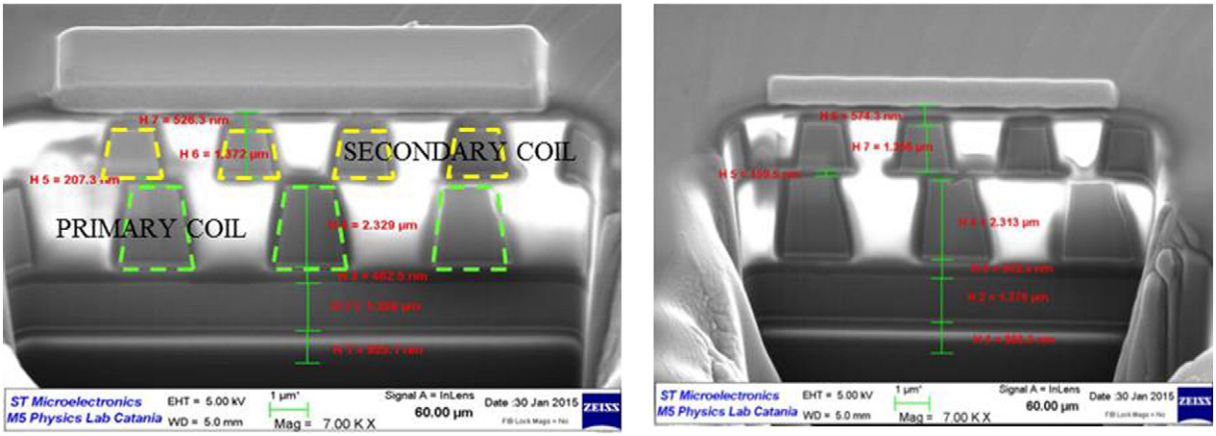

Fig. 3. SEM cross section images of the primary and secondary coils in different regions of the wafer.

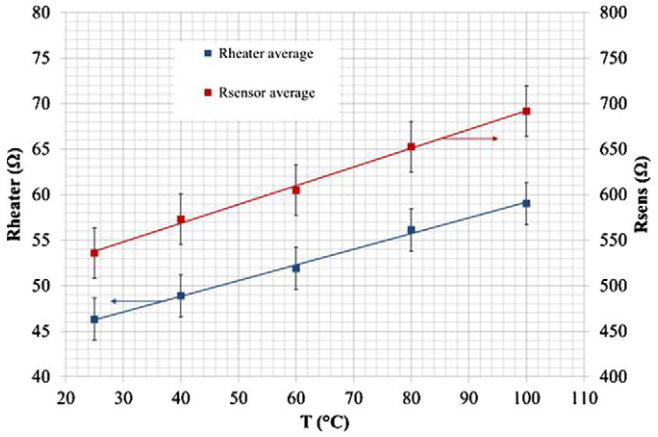

Fig. 4. Microheater and thermal sensor average resistance on wafer versus chuck temperature.

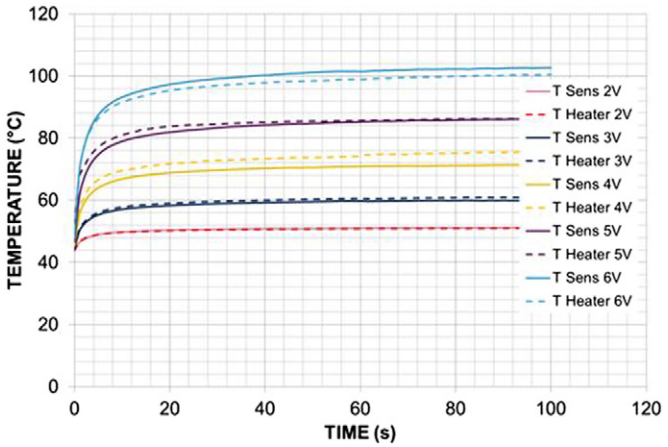

Fig. 6. Chip temperature extrapolated by micro-heater and thermal sensor currents.

Table 2
Heater and sensor average values and thermal coefficient.

Microheater resistance @ 0C	Sensor resistance @ 0C	Thermal coefficient
486 Ω	42 Ω	0.0041/C

microscopy image has been acquired by biasing the two micro-heaters in series: the temperature is uniform on the whole chip and the green and blue regions are an acquisition artifact due to the metals 2 and 3 low thermal emissivity coefficient.

In order to accurately evaluate the temperature of the chip on the PCB board we have biased the two micro-heaters in series at different voltages (from 2 to 6 V) and acquired the current flowing in the micro-heaters in the time. To confirm the data, we have biased the thermal sensor at 0.1 V (to avoid a contribution from the thermal sensor to the chip heating) and acquired the current on it extrapolating the temperature. The two extrapolated temperatures versus time are reported in Fig. 6. It can be noticed that the results are fully in agreement each other's, highlighting that the standard temperatures range usually used in biochemical reactions (70–90 °C) can be achieved just selecting the micro-heater driving voltage from 2 V to 6 V.

3.2. Magnetic components characterization

The sensor magnetic characterization has been based on the monitoring of differential output voltage at the secondary coils instead of the direct estimation of the inductance changes, upon the magnetic beads presence. This approach results more appropriate since the magnetic particles, acting as a moveable nucleus, create a direct relationship between the differential output voltage at the secondary coils and the number (or density) of magnetic particles. Therefore, a high-impedance detection of the differential output voltage at the secondary coils is a simple, but good, strategy in the detection of the magnetic particles.

The analysis of the response of the device has been measured on functionalized devices with magnetic beads. An amount of micromagnetic particles ranging from 12 ng to 250 ng were deposed by spotting (see Materials and Methods Section) on the surface of one of the two secondary coil. The correspondent secondary coils voltage signals, due to the magnetic field induced by the primary coil driven by a current signal of 7 mA @ 15 MHz, was recorded.

Commercially available, general-purpose discrete components and ICs have been used to realize the signal conditioning circuit for the proposed sensor.

The signal conditioning circuit has been designed to supply the primary winding with a sinusoidal current with constant amplitude, to detect and amplify the two peak voltages at the secondary coils and finally to produce an output signal proportional to the difference. A voltage-to-current converter is also required to provide the bias current such to be insensitive to the impedance changes at the primary coil.

In Fig. 7 the amplitude of the signal output as function of the plotted nanobeads concentration is reported. Solid line represents the sensor model, while dashed lines represent the uncertainly band.

From the plot of Fig. 7, a sensitivity of 5.1 mV/ng and a resolution of 0.0081 ng can be estimate. These data make the sensor very promising for biosensors applications based on nucleic acid or antibody–antigen detection. In addition, the possibility of temperature cycling make such a device compatible with biochemical reactions such us DNA amplification and hybridization process. Future development will be devoted to both set up of the biochemical strategy for DNA recognition

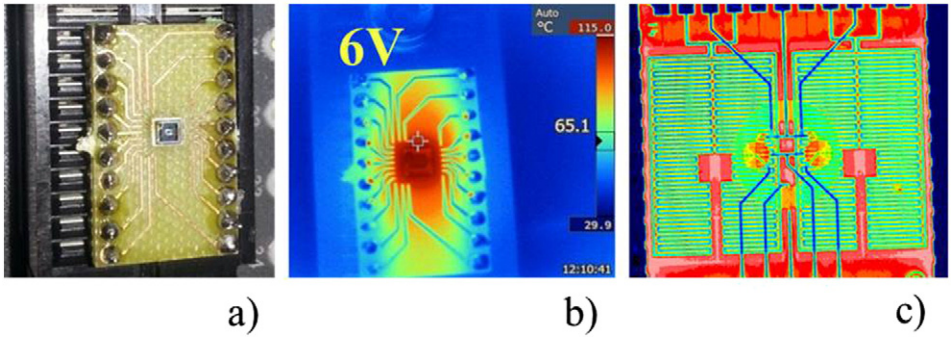

Fig. 5. Picture of the magnetic sensor mounted on a PCB (a), image acquired by a Fluke thermocamera (b) and a thermal microscopy image (c).

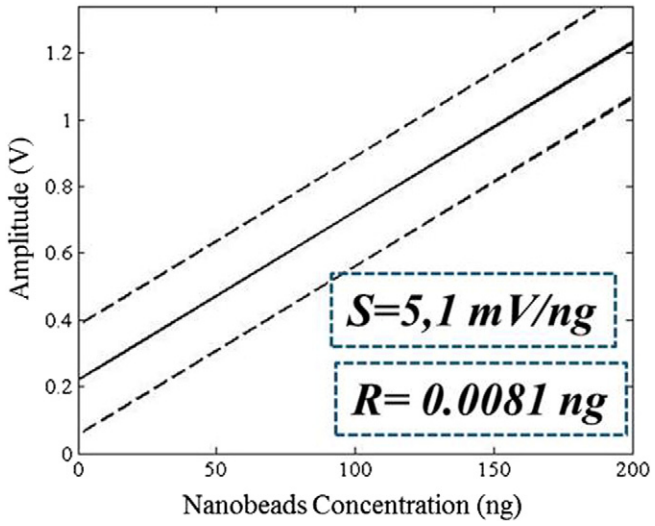

Fig. 7. Amplified differential output voltage of the transformer versus quantity of magnetic particles.

(primers and probes) and optimization of surface functionalization for the beads recognition. The advantages of this type of biosensor are: (i) many times faster than conventional PCR. (ii) more efficient in the number of DNA copies produced, (iii) easily designed to use small volumes, and (iv) save cost.

The application of the sensor as magnetic immunoassay has been proposed in [12]. We want to propose a method to detect nucleic acid. A schematic detection principle is sketched in Fig. 8.

The proposed principle requires thermal processes for primer extension and primer-probe hybridization and the functionalization of beads and of one secondary coil surfaces. Such functionalization consists of the coating of the sensors and particles surfaces with suitable materials to allow the binding of the suitable primer-probe. This can offers several advantages such as: (i) the signal detection is electrical and then can be integrated in compact devices; (ii) since the reading occurs at surface level, it is expected that few amount of extended beads are necessary to achieve measurable signals.

The device presented here can be considered a preliminary step toward the development of magnet RT-PCR (real time polymerase chain reaction) sensors.

4. Conclusion

A thermal-inductive device for biosensor application integrating both thermal and planar differential transformer configurations has been described in the present paper. The device allows both the detection of magnetic particles using a suitable signal conditioning circuit and the thermal driving function.

The ability of the sensor to detect and quantify the presence different amounts of micromagnetic particles has been proved. A sensitivity of 5.1 mV/ng and a resolution of 0.0081 ng have been calculated. Thermal behavior has been also demonstrated highlighting that the standard temperatures range usually used in biochemical reactions (25–90 °C) can be achieve just selected the micro-heater driving voltage.

The results here discussed are very promising for the development of low-cost, high-sensitivity, integrated magnetic biosensor systems application. Further investigations are in progress to evaluate the device performances by modifying some fundamental parameters such as bead sizes and surface chemistry.

Acknowledgments

This work has been funded by MIUR by means of the national Program PON R&C 2007–2013, project “Hyppocrates–Sviluppo di Micro e Nano-Tecnologie e Sistemi Avanzati per la Salute dell'uomo” (PON02 00355) and PRIN 2010–2011 “Metodologie chimiche innovative per biomateriali intelligenti”.

References

[1] R. Higuchi, G. Dollinger, P.S. Walsh, R. Griffith, Simultaneous amplification and detection of specific DNA sequences, Biotechnology 10 (1992) 413–417.
[2] J. Wilhelm, A. Pingoud, Real-time polymerase chain reaction, ChemBioChem 4 (2003) 1120–1128.
[3] B. Foglieni, A. Brisci, F.S. Biagio, P.P. Di Pietro, S. Petralia, S. Conoci, M. Ferrari, L. Fremonesi, Molecular diagnostics on a Lab-on-chip device. A new advanced solution for mutation detection in gene-diseases, Clin. Chem. Lab. Med. 48 (2010) 329–336.
[4] S. Libertino, S. Conoci, M.F. Santangelo, R. Pagano, E.L. Sciuto, F. Sinatra, D. Sanfilippo, G. Fallica, S. Lombardo, Optical and electrical Si-based biosensors: fabrication and trasduction issues, J. Anal. Bioanal. Tech. S12 (2014) 007, http://dx.doi.org/10.4172/2155-9872.S12-007.
[5] S. Libertino, S. Conoci, A. Scandurra, R.C. Spinella, Biosensor integration on Si-based devices: feasibility studies and examples, Sensors Actuators B Chem. 179 (2013) 240–251.
[6] S. Conoci, A. Mascali, F. Pappalardo, Synthesis, DNA binding properties and electrochemistry to an electrode-bound DNA of an novel anthracene-viologen conjugate, RSC Adv. 4 (2014) 2845–2850.
[7] S. Ghionea, P. Dhagat, A. Jander, Ferromagnetic resonance detection for magnetic microbead sensors, IEEE Sensors J. 8 (6) (2008) 896.
[8] C. Serre, S. Martìnes, A. Perez-Rodrìguez, J.R. Morante, J. Esteve, J.U. Montserrat, Si Technology bbased microinductive devices for biodetection applications, Sensors Actuators A 132 (3) (2006) 499–505.
[9] S. Baglio, S. Castorina, N. Savalli, Integrated inductive sensors for the detection of magnetic microparticles, IEEE Sensors J. 5 (3) (2005) 372–375.
[10] S. Dubus, B. Le Drogoff, J.F. Gravel, D. Boudreau, T. Veres, PCR-free DNA-based biosensing with polymeric optical hybridization transduction using micro- and submicron-magnetic bead captured on micro-electromagnetic traps, NSTI-Nanotech 2006, 2, ISBN: 0-9767985-7-3, 2006 (www.nsti.org).
[11] Steven M. Hira, Khaled Aledealat, Kan-Sheng Chen, Mark Field, Gerard J. Sullivan, P. Bryant Chase, Peng Xiong, Stephan von Molniar, F. Geoffrey, Strouse1, detection of target ssDNA using a microfabricated hall magnetometer with correlated optical readout, J. Biomed. Biotechnol. (2012) 492730.
[12] B.Andò, S. Baglio, A. Beninato, G. Fallica, V. Marletta, N. Pitrone, Analysis and Design of Inductive Biosensors for Magnetic Immunoassay, XIX IMEKO World Congress Fundamental and Applied Metrology September 6–11 (2009) Lisbon, Portugal.
[13] S.S. Mohan, M. del Mar Hershenson, S.P. Boyd, T.H. Lee, Simple accurate expressions for planar spiral inductances, IEEE J. Solid State Circuits 34 (10) (1999) 1419–1424.

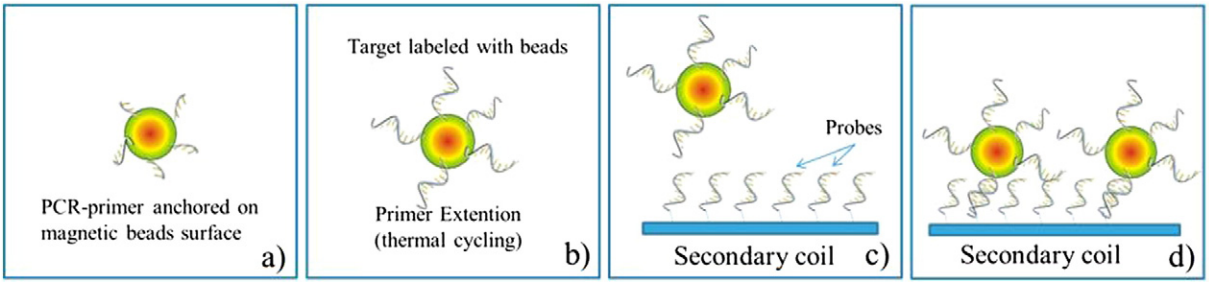

Fig. 8. Schematics of the detection principle. (a) The PCR primer is anchored on the functionalized beads surface. (b) Primer extension through thermal cycling. (c) Probe anchored on one of the two secondary coils. (d) Hybridization and then detection.